Journal of Power Sources 325 (2016) 646–652

Contents lists available at ScienceDirect

Journal of Power Sources

journal homepage: www.elsevier.com/locate/jpowsour

Nickel hexacyanoferrate, a versatile intercalation host for divalent ions from nonaqueous electrolytes

Albert L. Lipson, Sang-Don Han, Soojeong Kim, Baofei Pan, Niya Sa, Chen Liao, Timothy T. Fister, Anthony K. Burrell, John T. Vaughey, Brian J. Ingram*

Chemical Sciences and Engineering Division, Joint Center for Energy Storage Research, Argonne National Laboratory, 9700 S. Cass Ave., Lemont, IL, 60439, USA

HIGHLIGHTS

- Nickel hexacyanoferrate is shown to electrochemically insert Mg, Ca and Zn ions.
- Intercalation voltages are 2.9 V, 2.6 V, and 1.2 V for Mg, Ca and Zn, respectively.
- Changes to composition, structure, and iron oxidation state are observed.
- The electrochemistry is reversible.

ARTICLE INFO

Article history:
Received 27 January 2016
Received in revised form
4 May 2016
Accepted 5 June 2016
Available online 25 June 2016

Keywords:
Nickel hexacyanoferrate
Magnesium battery
Calcium battery
XANES
Nonaqueous

ABSTRACT

New energy storage chemistries based on Mg ions or Ca ions can theoretically improve both the energy density and reduce the costs of batteries. To date there has been limited progress in implementing these systems due to the challenge of finding a high voltage high capacity cathode that is compatible with an electrolyte that can plate and strip the elemental metal. In order to accelerate the discovery of such a system, model systems are needed that alleviate some of the issues of incompatibility. This report demonstrates the ability of nickel hexacyanoferrate to electrochemically intercalate Mg, Ca and Zn ions from a nonaqueous electrolyte. This material has a relatively high insertion potential and low overpotential in the electrolytes used in this study. Furthermore, since it is not an oxide based cathode it should be able to resist attack by corrosive electrolytes such as the chloride containing electrolytes that are often used to plate and strip magnesium. This makes it an excellent cathode for use in developing and understanding the complex electrochemistry of multivalent ion batteries.

1. Introduction

After many years of research, electric vehicles and grid storage are starting to be deployed using Li-ion batteries; however, mass market penetration has not been realized due to issues related to their cost, lifetime, and energy density. There are many possible avenues to reduce the cost of batteries, such as increasing the capacity and reducing the cost of raw materials [1]. By using a multivalent working ion, such as Mg or Ca, a battery with higher capacity and lower cost materials could potentially be made. In particular, these multivalent elements are substantially more abundant in the earth's crust as compared to Li, which results in them being considerably less expensive. Additionally, these systems can be designed to utilize a metal anode, which dramatically increases the capacity of the cell relative to the use of an intercalation host anode (e.g., graphite), thereby further reducing the system cost. Li-metal anodes have been explored for decades; however, there are still substantial challenges to commercialization related to dendrite formation, low coulombic efficiency, and high reactivity [2]. Mg metal anodes, on the other hand, are achievable and show improved plating properties relative to Li-metal [3]. Ultimately, Mg and other multivalent ions are predicted to provide a significant increase in volumetric energy density and reduction in cost relative to Li-ion technologies [4].

A successful rechargeable mutivalent battery requires a high capacity cathode that can support reasonable cycling rates. Many cathode materials for Mg intercalation have been explored

* Corresponding author.
E-mail address: ingram@anl.gov (B.J. Ingram).

http://dx.doi.org/10.1016/j.jpowsour.2016.06.019
0378-7753/

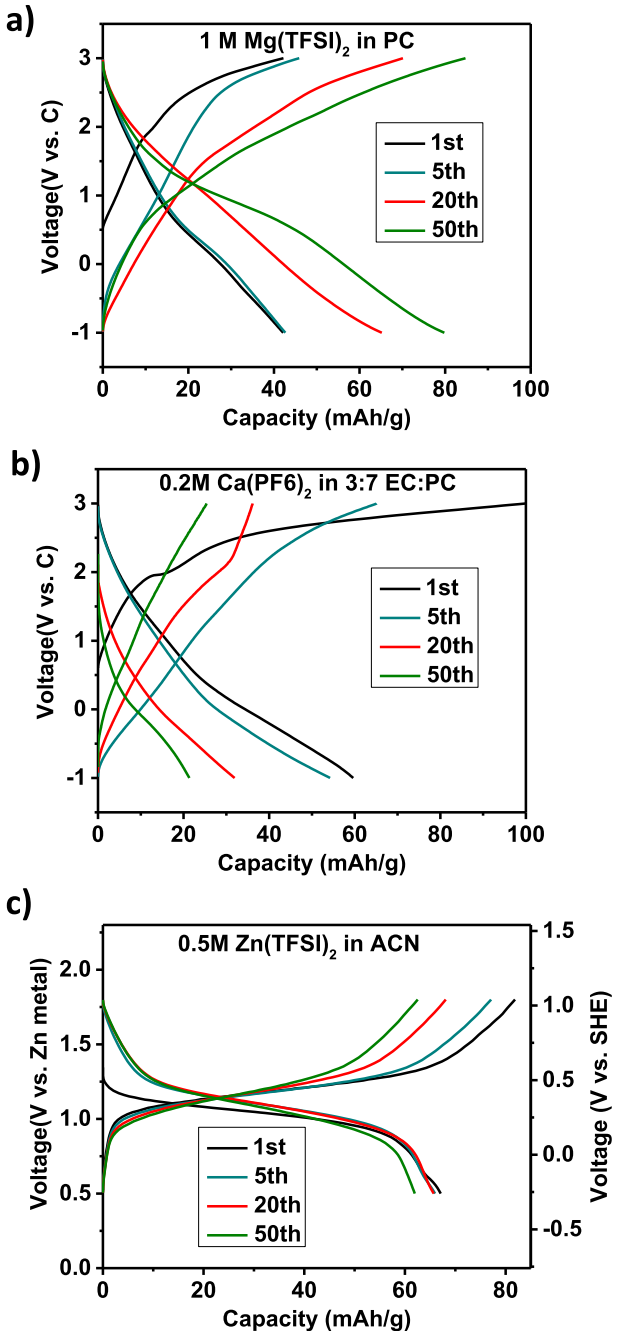

Fig. 1. Galvanostatic cycling (charging first, except for Zn) of multivalent ions at a rate of 10 mA g^{-1} with NFCN as the cathode. a) Using 1 M $Mg(TFSI)_2$ in PC as the electrolyte with a BP2000 carbon anode, b) using 0.2 M $Ca(PF_6)_2$ in 3:7 EC:PC with a BP2000 carbon anode, and c) using 0.5 M $Zn(TFSI)_2$ in ACN with a Zn metal anode.

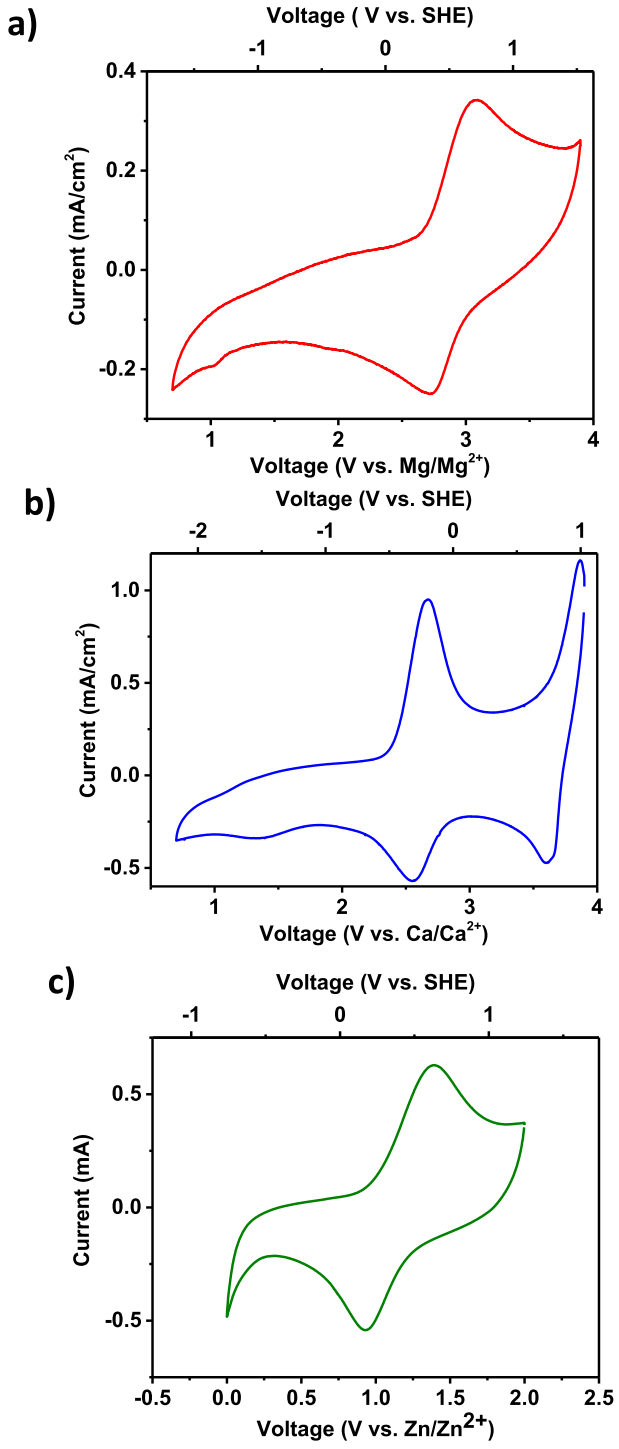

Fig. 2. Cyclic voltammograms for NFCN as the working electrode at a rate of 1 mV/s a) Using 1 M $Mg(TFSI)_2$ in PC as the electrolyte with a BP2000 carbon counter electrode and a Ca metal reference, b) using 0.2 M $Ca(PF6)_2$ in 3:7 EC:PC with a BP2000 carbon counter electrode and a Ca metal reference, and c) using 0.5 M $Zn(TFSI)_2$ in ACN with a Zn metal counter electrode and reference. Voltages for the Mg and Ca systems are converted to the standard potential using a ferrocene calibration.

including Mo_6S_8 (Chevrel) [3], V_2O_5 [5], λ-Mn_2O_4 [6], Prussian blue complexes [7–11], and many others [12,13]. Currently proposed Mg-ion intercalation cathodes typically exhibit low energy density, high overpotential, or they require high water content electrolytes to promote Mg insertion. For instance, Chevrel phase has a theoretical capacity of 129 mA h/g between 1 V and 1.3 V [3], which is less than one third of the voltage that is theoretically achievable in Li-ion systems. In the example of V_2O_5, only low intercalation capacity can be obtained unless substantial amounts of water are present in the electrolyte [14].

Prussian blue type complexes have been explored extensively for use in Na and Li based nonaqueous batteries [15–19], making them a promising candidate for use with multivalent ions. Prussian blue type complexes, such as barium hexacyanoferrate, copper hexacyanoferrate and nickel hexacyanoferrate (NFCN), have been shown to intercalate Ca, Mg and Zn, but only in high water content

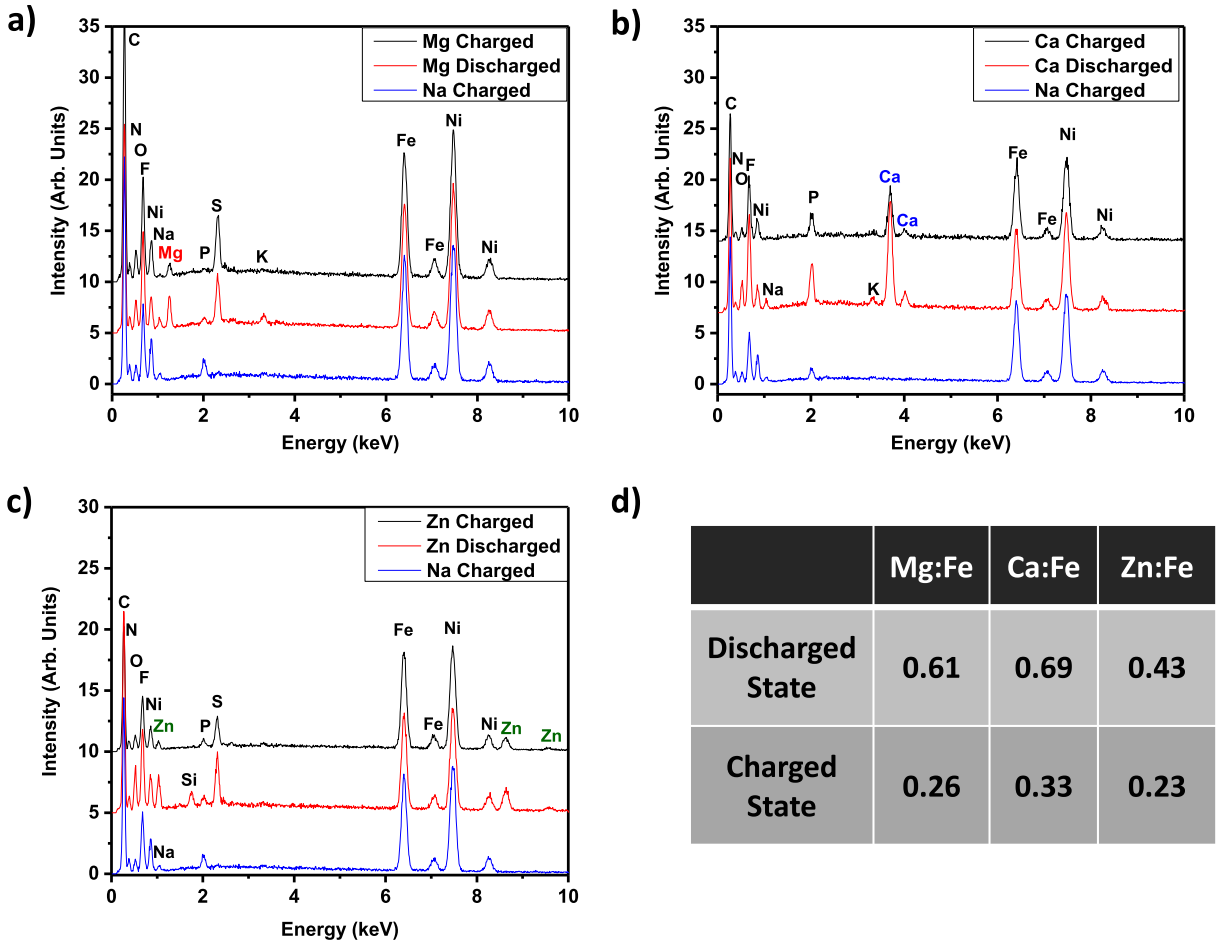

	Mg:Fe	Ca:Fe	Zn:Fe
Discharged State	0.61	0.69	0.43
Charged State	0.26	0.33	0.23

Fig. 3. EDX spectra for NFCN at different states of charge and with a) Mg, b) Ca, and c) Zn in the lattice. d) Table summarizing the compositional changes estimated by EDX in the charged and discharged states for the different ions.

electrolytes [7,8,20–22], which limits the voltage window of the device. Recently, we have shown that manganese hexacyanoferrate, with an analogous structure to NFCN, can intercalate Ca using a low water content nonaqueous electrolyte [11]. However, we have yet to see evidence that it can intercalate other multivalent ions. Furthermore, there have been no reports of a Prussian blue analogue that can intercalate Mg from a nonaqueous electrolyte.

Herein, we demonstrate that NFCN, which has an ideal stoichiometry of $NiFe(CN)_6$, can be used as an intercalation host for Mg, Ca and Zn using a low water content nonaqueous electrolyte. In particular, we establish the electrochemical cycling performance and intercalation voltage using a combination of cyclic voltammetry (CV) and galvanostatic cycling. Furthermore, we demonstrate that this electrochemical signal is caused by the intercalation of these species via a combination of energy dispersive X-ray spectroscopy (EDX), X-ray diffraction (XRD), and X-ray absorption near-edge structure (XANES) measurements.

2. Experimental

NFCN was prepared by a solution based method similar to Wang et al. [7] Specifically, 0.008 mol of $Ni(NO_3)_2$ (Hexahydrate, Fisher Scientific) in 70 mL of DI water were added dropwise to 0.004 mol of $Na_4Fe(CN)_6$ (Decahydrate, Sigma Aldrich) in 130 mL of DI water while stirring vigorously. After the addition was complete the solution was allowed to stir for 2 h before filtration to allow the reaction to come to completion. The solution was then filtered and the precipitate rinsed with DI water at least 3 times. The resulting material was dried at 75 °C in air. A slurry was then made with 80% NFCN, 10% Timcal Super C45 carbon black, and 10% Solvay Solef poly(vinylidene difluoride) with n-methyl-2-pyrrolidinone (Anhydrous, Sigma-Aldrich) as a solvent. The slurry was coated onto Graftech Grafoil graphite foil, dried at 75 °C in air and further dried at 75 °C under vacuum overnight. Electrodes at this state are termed “uncycled.” The electrodes used for further testing were electrochemically desodiated by charging to 3 V vs. a BP2000 carbon anode using 1 M $NaPF_6$ (Sigma Aldrich) in 1:1 ethylene carbonate (EC) (Sigma Aldrich) to propylene carbonate (PC) (anhydrous, Sigma Aldrich) electrolyte. The propylene carbonate was dried using molecular sieves for at least 12 h prior to use. The desodiated electrodes were rinsed thoroughly in dimethyl carbonate (DMC) and dried before being used in the Mg, Ca or Zn cells. Electrodes in this rinsed state are termed “Na charged.”

The electrolytes for Ca and Zn were chosen based on previous successful electrolytes [11,23]. The Mg electrolyte was chosen due to the commercial availability of the salt and the compatibility advantages of using a PC based electrolyte. Electrolyte preparation and cell fabrication were both done in an argon-filled glovebox with less than 1 ppm O_2 and H_2O. Mg based electrolyte was prepared from magnesium bis(trifluoromethane sulfonyl)imide ($Mg(TFSI)_2$) (99.5%, Solvionic, France) dried in a vacuum oven at 180 °C for 60 h before use. Propylene carbonate (Aldrich, anhydrous, 99.7%) solvent was pretreated with molecular sieves (Aldrich, 3 Å beads, 4–8 mesh) overnight and then added into the

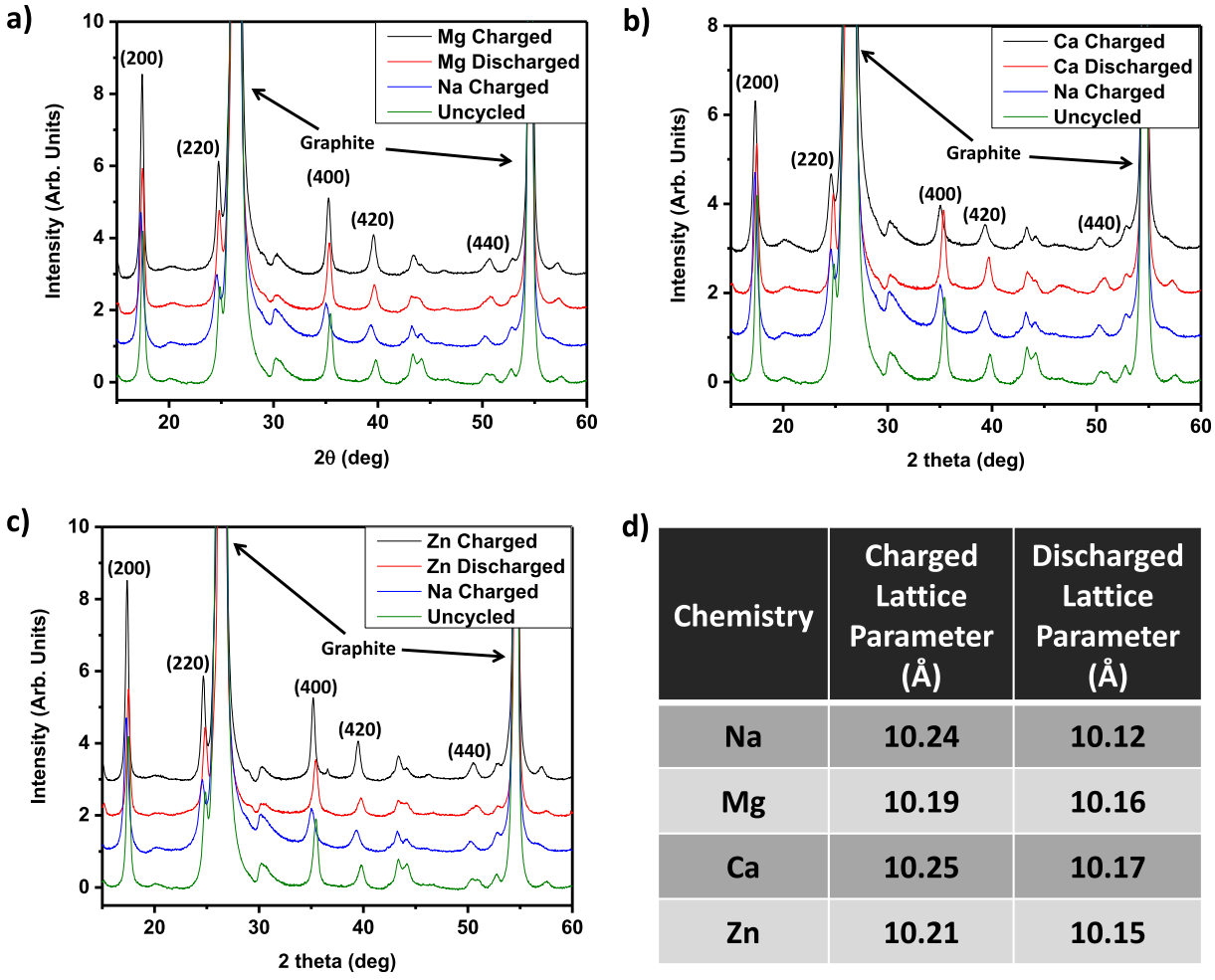

d)

Chemistry	Charged Lattice Parameter (Å)	Discharged Lattice Parameter (Å)
Na	10.24	10.12
Mg	10.19	10.16
Ca	10.25	10.17
Zn	10.21	10.15

Fig. 4. X-ray diffraction patterns for NFCN at different states of charge and with a) Mg, b) Ca, and c) Zn in the lattice. d) Table summarizing the lattice parameter changes in the charged and discharged states for the different ions.

dried $Mg(TFSI)_2$. The as prepared electrolyte was then stirred overnight before use. Water content of the as prepared Mg electrolyte was under 20 ppm, as determined from Karl-Fischer analysis using a Mettler Toledo DL39 Karl Fischer coulometer. $Ca(PF_6)_2$ based electrolyte was prepared as described previously [11]. Appropriate ratios of dried $Zn(TFSI)_2$ (Solvionic, 99.5%) and dried anhydrous acetonitrile (ACN) (Sigma-Aldrich, 99.8%) were mixed together in hermetically sealed glass vials and magnetically stirred to form homogeneous solutions of the Zn electrolyte, as reported previously [23]. The water content of this mixtures was confirmed to be <30 ppm via Karl Fischer titration.

Coin cells for cycling and 3-electrode Swagelok type cells were prepared using graphite spacers as have been described previously [24]. A Ca metal reference electrode was used for testing the Mg and Ca cells, with the voltage calibrated using ferrocene. In the Mg cells Mg metal cannot be used since the electrolyte forms a blocking layer on its surface, however, Ca is not completely blocked in this electrolyte allowing it to be used as a pseudoreference. Zn 3-electrode cells used a Zn metal reference with no further voltage modification, due to its stable and known voltage in the electrolyte [23]. Mg and Ca cells were cycled from −1 V to 3 V vs. a BP2000 carbon anode, and Zn cells were cycled from 0.3 V to 2 V vs. a Zn anode using a series 4000 Maccor cycler at 10 mA/g. Cyclic voltammetry was taken using a Princeton Instruments Parstat MC potentiostat. Cells that were charged and then discharged are termed “X discharged,” where X is Mg for cells using 1 M $Mg(TFSI)_2$ in PC, Ca for cells using 0.2 M $Ca(PF_6)_2$ in 3:7 EC:PC, and Zn is for cells using 0.5 M $Zn(TFSI)_2$ in ACN. If these cells in the discharged state are recharged the electrodes are termed “X charged.”

Ex situ characterization was performed after rinsing harvested electrodes thoroughly in DMC under an inert atmosphere. Energy dispersive X-ray spectroscopy (EDX) was taken using a Hitachi S4700-II scanning electron microscope equipped with an EDX detector from EDAX with 30 keV electrons. A Rigaku Miniflex 600 was used to take X-ray diffraction (XRD) patterns using Cu Kα radiation. The 2θ values were adjusted for height variation using $2\theta_f = 2\theta_o + \frac{2\delta}{L}\cos(\theta_o)$, where θ_f is the corrected value for θ, θ_o is the original value for θ, δ is the height displacement, and L is the camera length, such that the d-spacing for the (004) peak is exactly half of that for the (002) peak. XANES was taken at sector 10BM at the Advanced Photon Source at Argonne National Laboratory in transmission mode using nickel and iron metal energy references. Spectra were normalized using the Athena software package [25].

3. Results and discussion

The electrochemical performance of the NFCN material was studied via galvanostatic cycling using coin cells. Prior to galvanostatic cycling NFCN was electrochemically desodiated and rinsed before reassembly. This desodiation step changes the Na content

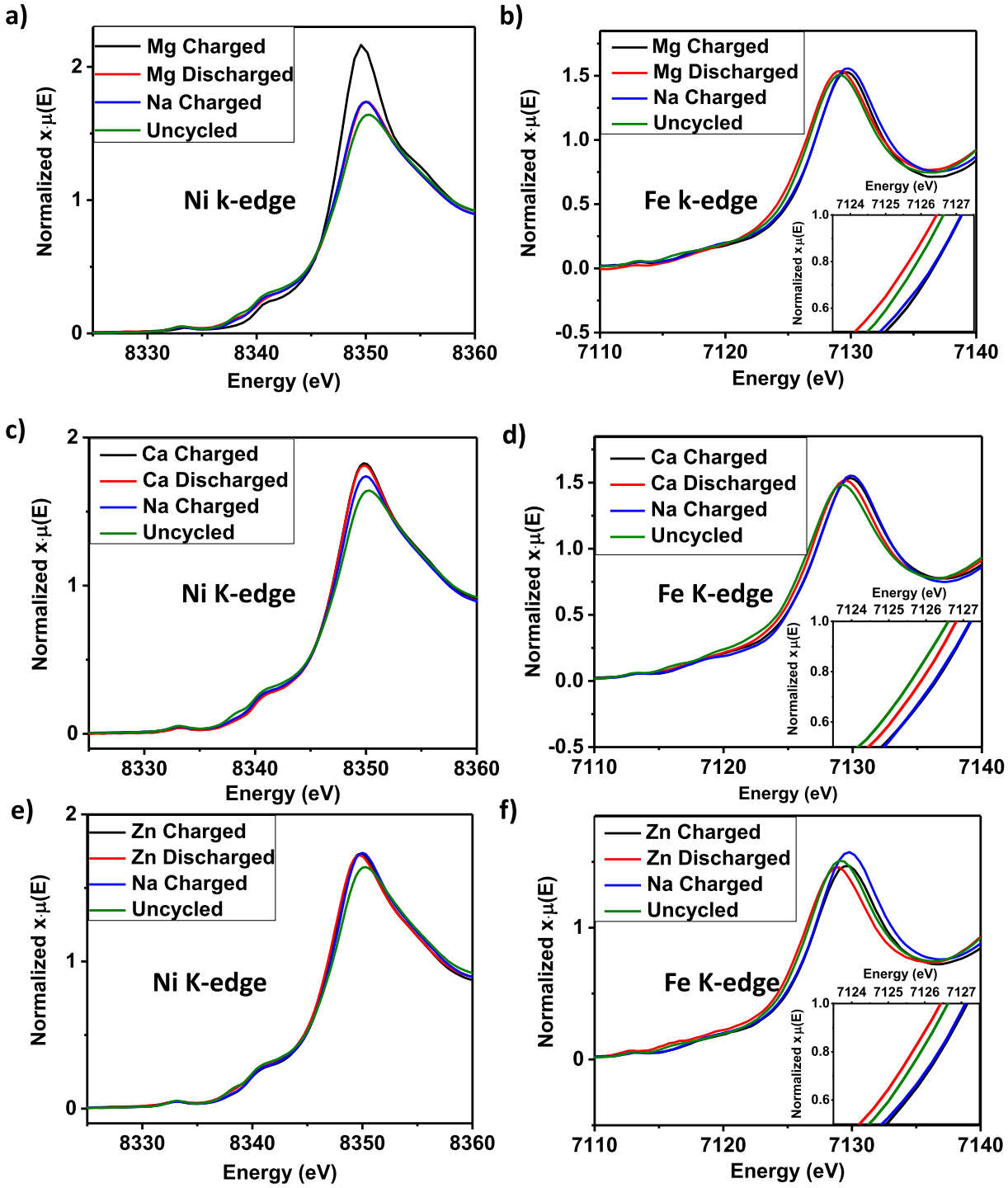

Fig. 5. XANES spectra for a,b,c) the Ni K-edge and d,e,f) the Fe K-edge for NFCN samples at various states of charge and with Mg, Ca and Zn as insertion ions.

according to EDX from 0.66 to 0.22 Na:Fe ratio. A comparison of the cycling behavior of these previously electrochemically desodiated NFCN electrodes with different ions are shown in Fig. 1. It should be noted that the Mg and Ca samples were cycled against a capacitive carbon anode to avoid compatibility issues with a metal anode, whereas the Zn sample was cycled against Zn metal. The capacities in all three electrolytes are similar to the capacities seen in Na and aqueous batteries (~50 mA h/g) [7,15,18]. The capacity and voltage behavior variations with cycling are dependent on the chemistry. In particular, the response of the Mg and Ca systems investigated are opposite with respect to capacity retention upon cycling. 1.0 M $Mg(TFSI)_2$ in PC shows a capacity increases from 40 to 80 mA h/g after 50 cycles, which can be attributed to decomposition of the TFSI anion that subsequently reacts electrochemically to increase the capacity [26]. With the Ca electrolyte (0.2 M $Ca(PF_6)_2$ in 3:7 EC:PC), however, capacity fades substantially with cycling. We notice that cells using this Ca-based electrolyte have very little liquid electrolyte remaining after cycling, which we believe to be caused by the lack of a good passivation layer causing the electrolyte to be consumed during cycling. Finally, with 0.5 M $Zn(TFSI)_2$ in

ACN the capacity is reasonably stable over 50 cycles, because the TFSI anion is more stable in this voltage range. This cycling data indicates that an apparently reversible electrochemical reaction is occurring in all 3 systems, but does not prove either intercalation or in the case of Mg and Ca the voltage of the electrochemical reaction.

In order to determine the voltage of the electrochemical reactions, we utilized cyclic voltammetry in three-electrode cells using a ferrocene calibrated Ca pseudoreference for the Mg and Ca electrolytes and a Zn metal reference for the Zn electrolyte. In the Mg chemistry only one reversible reaction is apparent at about 2.9 V vs. Mg/Mg^{2+} (Fig. 2a). Ca, however, shows 2 distinct reversible reactions at 2.6 V and 3.7 V vs. Ca/Ca^{2+} (Fig. 2b). The reaction at 2.6 V is likely due to the $Fe^{2+/3+}$ couple and at 3.7 V likely due to the $Ni^{2+/3+}$ redox couple. Due to the high voltage nature of the $Ni^{2+/3+}$ redox couple, it is unlikely that Ni can be oxidized in the electrolytes used in these cells during galvanostatic cycling. Similar to Mg, Zn shows a single reversible reaction at 1.2 V vs. Zn/Zn^{2+} (Fig. 2c), which is almost the same voltage as Mg vs. a standard hydrogen electrode (0.5 V for Mg vs. 0.4 V for Zn). The Zn CV also shows an apparent reduction reaction occurring at just above 0 V, which is likely due to surface film formation and not Zn plating as this peak is irreversible.

EDX analysis, shown in Fig. 3, was used to estimate elemental composition evolution during the cycling processes. In all of the chemistries there is an apparent increase in the content of Mg, Ca or Zn upon discharge. When the cell is subsequently charged the peaks corresponding to the active ions are reduced, thereby indicating that the working ions can be removed from the cathode. It should be noted, that since the charged sample has undergone additional cycling as compared to the discharged sample this change in composition is unlikely to be caused by surface film growth. All samples contain a small amount of P from the desodiation step using $NaPF_6$. The samples that were cycled using TFSI-based electrolytes (Mg and Zn) show a substantial amount of S, which is a surface film created by decomposition of the TFSI anion. Ca charged and discharged samples show an increased concentration of P as compared to the desodiated sample, indicating further surface film formation on the cathode or partial intercalation of a P containing ion. Quantification of the stoichiometry shows that approximately 0.7, 0.7, and 0.4 electrons per iron are being cycled for Mg, Ca and Zn respectively. This would imply a capacity of 70 mA h/g, 70 mA h/g and 40 mA h/g, respectively, assuming an initial stoichiometry of $Na_{0.45}NiFe(CN)_6$. These capacities are similar to what is found electrochemically with some amount of error, which is likely due to the inaccuracies in EDX quantification. However, EDX does not prove whether these ions are actually inserting into the NFCN versus undergoing a conversion reaction.

X-ray diffraction was used to monitor the structural changes at different states of charge, to see if the compositional fluctuations, shown in Fig. 3, are caused by the active ions intercalating into the NFCN. The resulting XRD patterns are shown in Fig. 4. Upon discharge, which corresponds to the insertion of the active ion, there is a contraction of the lattice, due to the Fe-C spacing in the hexacyanoferrate ion shrinking when the Fe oxidation state is decreased [7,27]. Subsequent charging of the NFCN results in partial lat tice expansion for all of the chemistries. However, only in the case of Ca does the lattice return close to the desodiated state. This is likely caused by some Mg and Zn remaining in the lattice after charging. The discharged lattice parameter for all the chemistries is larger than that seen in the uncycled case, which is probably due to the high charge density of the multivalent ions preventing contraction of the lattice. The overall expansion and contraction even for Ca is less than 1%, indicating that the NFCN is unlikely to undergo mechanical degradation during cycling due to this effect.

Intercalation further requires that the host transition metals change oxidation states to compensate for the charge of the intercalating ion. In order to study the changes in the bulk oxidation state of the Ni and Fe in the NFCN material, XANES spectra were taken in transmission mode as shown in Fig. 5. In general the Ni K-edge shows an initial slight reduction in edge energy indicating a reduction of the Ni oxidation state, which is attributed to the nickel redox potential being outside the electrolyte stability window causing the electrolyte to oxidize and the nickel to reduce. There is also a substantial change in the white line intensity (peak in the absorption) for the Mg charged sample, which can be attributed to the Ni attaining a more symmetric coordination environment for this sample [28]. More interestingly, the Fe K-edge appears to shift with the state of charge of the electrodes. In particular, the removal of sodium causes a shift to higher energies of approximately 0.5 eV, indicating about 0.5 electrons transferred.[29] During discharge the edge shifts back to a position very close to the uncycled state for Mg, Ca and Zn samples. This reveals that the iron oxidation state is reduced by about 0.5. Upon recharging the edge returns to the position of the Na charged state, thereby demonstrating the reversibility of the process. These changes in iron oxidation state would imply an approximate capacity of 50 mA h/g, which is consistent with the cycling performance.

4. Conclusion

NFCN has been shown to be able to insert Mg, Ca and Zn ions electrochemically from nonaqueous electrolytes. The cycling performance indicates an initial capacity of about 40, 60 and 50 mA h/g for Mg, Ca and Zn, respectively. The voltages of intercalation found using cyclic voltammetry were 2.9 V vs. Mg/Mg^{2+}, 2.6 V vs. Ca/Ca^{2+} and 1.2 V vs. Zn/Zn^{2+} for Mg, Ca and Zn intercalation, respectively. Characterization using EDX, XRD and XANES indicate changes to the composition, structure and iron oxidation state that are consistent with intercalation at these capacities. Although the capacity of this material is too low to be used in practical batteries, it provides a stable structure that can intercalate a wide range of ions from nonaqueous electrolytes. This will allow for studies to better understand the full cell interactions in Mg, Ca and Zn electrochemistry and thereby help enable practical implementation of Mg, Ca or Zn batteries.

Acknowledgements

This work was supported as part of the Joint Center for Energy Storage Research, an Energy Innovation Hub funded by the U.S. Department of Energy, Office of Science, Basic Energy Sciences. We would also like to acknowledge the u*se of the Center for Nanoscale Materials, supported by the* U. S. Department of Energy, Office of Science, Office of Basic Energy Sciences, *under Contract No. DE-AC02-06CH11357.* MRCAT (APS sector 10BM) operations are supported by the Department of Energy and the MRCAT member institutions. This research used resources of the Advanced Photon Source, a U.S. Department of Energy (DOE) Office of Science User Facility operated for the DOE Office of Science by Argonne National Laboratory under Contract No. DE-AC02-06CH11357.

References

[1] K.G. Gallagher, S. Goebel, T. Greszler, M. Mathias, W. Oelerich, D. Eroglu, V. Srinivasan, Energy Environ. Sci. 7 (2014) 1555–1563.
[2] Z. Li, J. Huang, B. Yann Liaw, V. Metzler, J. Zhang, J. Power Sources 254 (2014) 168–182.
[3] D. Aurbach, Z. Lu, A. Schechter, Y. Gofer, H. Gizbar, R. Turgeman, Y. Cohen, M. Moshkovich, E. Levi, Nature 407 (2000) 724–727.
[4] R. Van Noorden, Nature 507 (2014) 26–28.
[5] W. Yu, D. Wang, B. Zhu, G. Zhou, Solid State Commun. 63 (1987) 1043–1044.
[6] C. Kim, P.J. Phillips, B. Key, T. Yi, D. Nordlund, Y. Yu, R.D. Bayliss, S. Han, M. He,

Z. Zhang, A.K. Burrell, R.F. Klie, J. Cabana, Adv. Mater. 27 (2015) 3377–3384.
[7] R.Y. Wang, C.D. Wessells, R.A. Huggins, Y. Cui, Nano Lett. 13 (2013) 5748–5752.
[8] R.Y. Wang, B. Shyam, K.H. Stone, J.N. Weker, M. Pasta, H. Lee, M.F. Toney, Y. Cui, Adv. Energy Mater. 5 (2015) 1401869, http://dx.doi.org/10.1002/aenm.201401869.
[9] D.-M. Kim, Y. Kim, D. Arumugam, S.W. Woo, Y.N. Jo, M.-S. Park, Y.-J. Kim, N.-S. Choi, K.T. Lee, ACS Appl. Mater. Interfaces 8 (2016) 8554–8560.
[10] C. Ling, J. Chen, F. Mizuno, J. Phys. Chem. C 117 (2013) 21158–21165.
[11] A.L. Lipson, B. Pan, S.H. Lapidus, C. Liao, J.T. Vaughey, B.J. Ingram, Chem. Mater. 27 (2015) 8442–8447.
[12] P. Saha, M.K. Datta, O.I. Velikokhatnyi, A. Manivannan, D. Alman, P.N. Kumta, Prog. Mater. Sci. 66 (2014) 1–86.
[13] H.D. Yoo, I. Shterenberg, Y. Gofer, G. Gershinsky, N. Pour, D. Aurbach, Energy Environ. Sci. 6 (2013) 2265–2279.
[14] P. Novák, J. Desilvestro, J. Electrochem. Soc. 140 (1993) 140–144.
[15] C.H. Li, Y. Nanba, D. Asakura, M. Okubo, D.R. Talham, R. Soc, Chem. Adv. 4 (2014) 24955–24961.
[16] L. Wang, Y. Lu, J. Liu, M. Xu, J. Cheng, D. Zhang, J.B. Goodenough, Angew. Chem. Int. Ed. 52 (2013) 1964–1967.
[17] S. Yu, M. Shokouhimehr, T. Hyeon, Y. Sung, ECS Electrochem. Lett. 2 (2013) A39–A41.
[18] Y. Shenglan, L. Yong, L. Yunhao, X. Ben, W. Qiuting, Y. Mi, J. Yinzhu, J. Power Sources 275 (2015) 45–49.
[19] Y. You, X. Wu, Y. Yin, Y. Guo, Energy Environ. Sci. 7 (2014) 1643–1647.
[20] Y. Mizuno, M. Okubo, E. Hosono, T. Kudo, H. Zhou, K. Oh-ishi, J. Phys. Chem. C 117 (2013) 10877–10882.
[21] Z. Jia, B. Wang, Y. Wang, Mater. Chem. Phys. 149–150 (2015) 601–606.
[22] R. Trócoli, F. La Mantia, ChemSusChem 8 (2015) 481–485.
[23] S. Han, N.N. Rajput, X. Qu, B. Pan, M. He, M.S. Ferrandon, C. Liao, K.A. Persson, A.K. Burrell, ACS Appl. Mater. Interfaces (2016), http://dx.doi.org/10.1021/acsami.1025b10024.
[24] A.L. Lipson, D.L. Proffit, B. Pan, T.T. Fister, C. Liao, A.K. Burrell, J.T. Vaughey, B.J. Ingram, J. Electrochem. Soc. 162 (2015) A1574–A1578.
[25] B. Ravel, M. Newville, J. Synchrotron Radiat. 12 (2005) 537–541.
[26] N.N. Rajput, X. Qu, N. Sa, A.K. Burrell, K.A. Persson, J. Am. Chem. Soc. 137 (2015) 3411–3420.
[27] A. Dostal, G. Kauschka, S.J. Reddy, F. Scholz, J. Electroanal. Chem. 406 (1996) 155–163.
[28] K.I. Pandya, R.W. Hoffman, J. McBreen, W.E. O'Grady, J. Electrochem. Soc. 137 (1990) 383–388.
[29] A. Bianconi, M. Dell'Ariccia, P.J. Durham, J.B. Pendry, Phys. Rev. B 26 (1982) 6502–6508.